Coupling Between Guided Surface Waves, Lateral Waves, and the Radiation Fields by Rough Surfaces—Full-Wave Solutions

EZEKIEL BAHAR, SENIOR MEMBER, IEEE

Abstract—**In this paper explicit expressions are presented for the guided surface waves and lateral waves that are excited when radiation fields are incident upon rough surfaces. Similarly, expressions are presented for the radiation fields scattered by rough surfaces that are excited by surface waves and lateral waves. In addition, coupling between the surface waves and the lateral waves due to surface irregularities is considered in detail.**

The solutions, which are based on a full-wave approach to the problem, are subject to the exact boundary conditions at the irregular interface. These are shown to be consistent with the reciprocity relationship in electromagnetic theory.

The validity of the approximate impedance boundary condition is examined and consideration is given to excitation at the grazing incidence, the Brewster angle, and to waves incident at the critical angle for total internal reflection. Optimum conditions are determined for coupling between the radiation fields, the surface waves, and the lateral waves incident upon irregular boundaries. Thus this work is applicable to problems of radio wave propagation near an irregular interface between two media and excitation of guided waves by irregular dielectric structures.

I. Introduction

RADIO WAVE PROPAGATION over irregular surfaces with variable electromagnetic parameters has been investigated extensively. The methods used to analyze this problem vary considerably and the results significantly depend upon the approximate assumptions made to simplify the derivations. Thus, for instance, employing the Rayleigh hypothesis, the scattered fields are represented by a discrete spectrum of upward traveling waves [1], and, using the Kirchoff approximations, the physical optics solutions are obtained by characterizing the irregular boundary by the Fresnel reflection coefficient for the local tangent plane [2].

The solutions derived in this paper are based on a full-wave approach [3], [4]. Thus the total fields are expressed in terms of a complete spectrum of upward and downward traveling radiation fields, lateral waves, and surface waves. At the irregular boundary, the total fields are subjected to the exact boundary conditions. Since the individual terms in the complete field expansions do not satisfy the boundary conditions for irregular surfaces, uniform convergence of the field expansions cannot be assumed. Thus using the full-wave approach, Green's theorem is employed to avoid term by term differentiation of the field expansions. An approximate impedance boundary condition has also been considered in detail and the full-wave solutions have been compared with earlier solutions to this problem [5], [6].

In this paper, explicit full-wave solutions are given for the guided surface waves and lateral waves excited by plane waves incident upon rough surfaces. These solutions are provided in a form that can readily be used by engineers who are not familiar with the analytic techniques used in their derivation. They can also be applied to periodic and random rough surfaces [5], [6]. Since the scattered radiation fields, due to incident plane waves, vanish as the transmitter or receiver approach the surface of the irregular boundary, the surface waves and the lateral waves constitute the dominant contribution to the total fields near the boundary.

Coupling between the surface waves and the lateral waves propagating over irregular boundaries is considered in detail. The region of the irregular surface where maximum coupling occurs between the lateral and the surface waves is determined.

The full-wave solutions are shown to be consistent with the reciprocity relationship in electromagnetic theory. Thus plots of the scattered surface waves and lateral waves as functions of the incident angle of the plane waves also represent the scattered radiation pattern for an irregular surface excited by incident surface waves and lateral waves.

Several illustrative examples are given in Section V with special consideration given to excitation at the grazing incidence, the Brewster angle, and the critical angle for total internal reflection. The validity of the approximate impedance boundary condition is also examined.

II. Full-Wave Solutions for the Scattered Surface Waves Excited by Line Sources at Large Distances from a Rough Surface and the Reciprocal Problem

A line source at large distances above a rough surface will excite scattered radiation fields as well as guided surface waves [4]. Since the scattered radiation field approaches zero as the observation point approaches the surface, $\theta_0^f \to \pi/2$, the surface wave is the dominant term near the interface $y = h(x)$. The coupling of plane waves into surface (guided) waves of the structure by surface irregularities is

Manuscript received June 2, 1976; revised April 25, 1977. This work was supported in part by the National Science Foundation and in part by the US Army Research Office.

The author is with the Electrical Engineering Department, University of Nebraska, Lincoln, NE 68588.

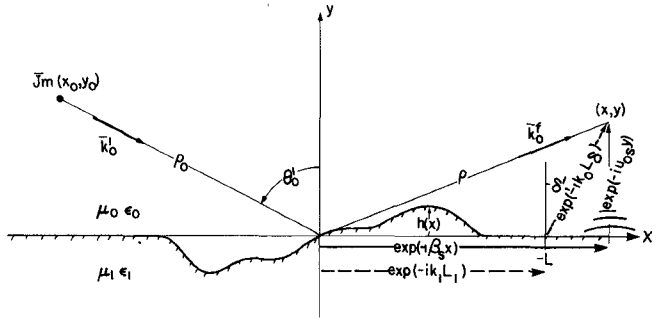

Fig. 1. The scattered surface waves and lateral waves due to incident plane waves over a rough surface.

also relevant to problems of coupling into and out of dielectric waveguides.

On expressing the electromagnetic fields in terms of generalized Fourier transforms and imposing exact boundary conditions at the irregular boundary [3], [4], it can be shown that the scattered vertically polarized surface wave at (x,y) due to a magnetic line source of intensity K (volts) located at (x_0,y_0) in medium 0 (Fig. 1) is

$$H^s_{zr}(x,y) = |H^i_0| \exp[-ik_0\rho_0]\left(\frac{i\omega}{\omega_c}\right)^{1/2} 4ik_0 LF(C_s,C^i) \cdot I(C_s,C^i,h,L)\exp[-i(\beta_s x + u_{0s}y)] \quad (2.1a)$$

$$F(C_s,C^i) = \frac{C^i_1 C_{1s} - S^i_0 S_{0s}}{(C^i_0 + C^i_1/n)n(1+1/\varepsilon_r)} \quad (2.1b)$$

and

$$I(C_s,C^i,h,L) = \frac{1}{2L}\int_{-L}^{L} \exp[iu^i_0 h + i(\beta_s - \beta^i)x]\,dx. \quad (2.1c)$$

An $\exp(i\omega t)$ time dependence is assumed and $|H^i_0|$ is the magnitude of the unperturbed incident wave at the origin:

$$|H^i_0| = K\omega_c\varepsilon_0/2[2\pi k_{0c}\rho_0]^{1/2}. \quad (2.1d)$$

The irregular deterministic boundary is given by (Fig. 1)

$$y = h(x), \qquad -L \le x \le L \quad (2.2a)$$

and $\rho_0 = (x_0^2 + y_0^2)^{1/2} \gg 1$ is the distance from the magnetic line source to the origin. The wavenumbers for media 0 and 1 are

$$k = \begin{cases} k_0 = \omega(\mu_0\varepsilon_0)^{1/2}, & y > h \\ k_1 = \omega(\mu_1\varepsilon_1)^{1/2}, & y < h \end{cases} \quad (2.2b)$$

and k_{0c} is the wavenumber at the carrier frequency ω_c. It is assumed here that μ and ε are not functions of x and $\mu_1 = \mu_0$. The complex refractive index is

$$n = \sqrt{\varepsilon_r} = \sqrt{\varepsilon_1/\varepsilon_0}. \quad (2.3)$$

The surface wave parameters are solutions to the modal equation

$$u_{0s}\varepsilon_1 + u_{1s}\varepsilon_0 = 0, \qquad \mathrm{Im}\,(u_{0,1}) < 0 \quad (2.4a)$$

thus

$$\beta_s = k_0 S_{0s} = k_1 S_{1s} = k_0\sqrt{\frac{\varepsilon_r}{1+\varepsilon_r}}$$

$$u_{0s} = k_0 C_{0s} = \frac{-k_0}{\sqrt{1+\varepsilon_r}}$$

$$u_{1s} = k_1 C_{1s} = k_1\sqrt{\frac{\varepsilon_r}{1+\varepsilon_r}} \quad (2.4b)$$

and for a plane wave incident at angle θ^i_0 in medium 0

$$\beta^i = k_{0,1}S^i_{0,1} = k_{0,1}\sin\theta^i_{0,1}$$

$$u^i_{0,1} = k_{0,1}C^i_{0,1} = k_{0,1}\cos\theta^i_{0,1}. \quad (2.4c)$$

For a plane wave at grazing incidence $\theta^i_0 \to \pi/2$ and $\omega = \omega_c$

$$|F(C_s,C^i_0 = 0)|_{\omega_c} = \left|\left[\left(1 - \frac{1}{\varepsilon_r}\right)^{1/2} - 1\right]\varepsilon_r^2/(\varepsilon_r^2 - 1)^{1/2}(\varepsilon_r + 1)\right|_{\omega_c}. \quad (2.5a)$$

In this work it is convenient to normalize F such that

$$F_N(C_s,C^i) = F(C_s,C^i)/|F(C_s,0)|_{\omega_c}. \quad (2.5b)$$

Thus in (2.1a), the input term $|H^i_0|\exp[-ik_0\rho_0]$ is the incident radiation field and the output term $\exp[-i(\beta_s x + u_s y)]$ is the scattered surface wave (see Fig. 1). The coupling phenomenon is represented by $F(C_s,C^i)$, which is a function of the angle of incidence and the ground parameters only, and $I(C_s,C^i,h,L)$, which is the only term that depends on the expression for the rough surface $h(x)$.

Similarly it can be shown that for backward-traveling surface waves of complex magnitude H_{s0} at the origin, the scattered radiation field at the observation point x,y is

$$H^r_{zs}(x,y) = H_{s0}\left(\frac{i\omega}{\omega_c}\right)^{1/2} 2k_{0c}Ln(1 - 1/\varepsilon_r^2) \cdot F(C^f,C_s)I(C^f,C_s,h,L)\frac{\exp[-ik_0\rho]}{[2\pi k_{0c}\rho]^{1/2}} \quad (2.6a)$$

where H_{s0}, the amplitude of the incident (unperturbed) surface waves at the origin, is [3]

$$H_{s0} = H_s(0,0) = Ki\omega\varepsilon_0 \exp[-i(\beta_s x_0 + u_{0s}y_0)]/n(1 - 1/\varepsilon_r^2) \quad (2.6b)$$

and

$$F(C^f,C_s) = \frac{C^f_1 C_{1s} + S^f_0 S_{0s}}{(C^i_0 + C^i_1/n)n(1+1/\varepsilon_r)} \quad (2.6c)$$

$$F_N(C^f,C_s) = F(C^f,C_s)/|F(0,C_s)|_{\omega_c} \quad (2.6d)$$

$$I(C^f,C_s,h,L) = \frac{1}{2L}\int_{-L}^{L} \exp[iu^f_0 h + i(\beta_s + \beta^f)x]\,dx. \quad (2.6e)$$

Equation (2.6a) reduces to (2.1b) on interchanging the locations of the source and the receiver. Thus

$$\rho_0 \to \rho \qquad x \to x_0 \qquad y \to y_0 \qquad \theta^i_0 \to -\theta^f_0 \quad (2.7)$$

and the results are consistent with reciprocity relationships in electromagnetic theory. As a consequence, the plot of the scattered surface wave as a function of θ_0^i (2.1a) is the same as the plot of the scattered radiation field as a function of θ_0^f (2.6a). In (2.6a), the input term is H_{s0}, the incident surface wave, and the output term is $\exp[-ik\rho]/[2k_{0c}\rho]^{1/2}$, corresponding to the scattered radiation field. The expression between these two terms represents the coupling phenomenon.

Using the approximate impedance boundary condition [5], the expression for the scattered surface wave due to a magnetic line source at (x_0,y_0) is also of the form (2.1b) except that here [5], [6]

$$F(C_s,C^i) = z_s S_{0s}(S_{0s} - S_0^i)/(C_0^i + z_s)(1 - z_s^2)^{1/2} \quad (2.8a)$$

and

$$|F(C_s,C_0^i = 0)|_{\omega_c} = |(1 - z_s^2)^{1/2} - 1|_{\omega_c}$$
$$F_N(C_s,C^i) = F(C_s,C^i)/|F(C_s,0)|_{\omega_c} \quad (2.8b)$$

where z_s is the normalized surface impedance

$$z_s = Z_s/\eta_0 \to (\varepsilon_r - 1)^{1/2}/\varepsilon_r, \qquad \text{Im}\,(z_s) > 0 \quad (2.9a)$$

and the surface-wave parameters are solutions of the modal equation

$$u_{0s} = -k_0 z_s. \quad (2.9b)$$

Thus

$$\beta_s = k_0 S_{0s} = k_0(1 - z_s^2)^{1/2}, \qquad \text{Im}\,(\beta_s) < 0$$

and

$$u_{0s} = k_0 C_{0s} = -k_0 z_s, \qquad \text{Im}\,(u_{0s}) < 0. \quad (2.9c)$$

The corresponding expression for the scattered radiation field due to an incident surface wave of complex amplitude H_{s0} at the origin is

$$H_{zs}^r(x,y) = H_{s0}\left(\frac{i\omega}{\omega_c}\right)^{1/2} 2k_{0c}L\frac{(1 - z_s)^{1/2}}{z_s}$$
$$\cdot F(C^f,C_s)I(C^f,C_s,h,L)\frac{\exp[-ik_0\rho]}{[2\pi k_{0c}\rho]^{1/2}} \quad (2.10a)$$

in which

$$H_{s0} = H_s(0,0)$$
$$= \frac{Ki\omega\varepsilon_0 z_s}{(1 - z_s^2)^{1/2}}\exp[-i(\beta_s x_0 + u_{0s}y_0)] \quad (2.10b)$$

$$F(C^f,C_s) = z_s S_{0s}(S_{0s} + S_0^f)/(C_0^f + z_s)(1 - z_s^2)^{1/2} \quad (2.10c)$$

$$F_N(C^f,C_s) = F(C^f,C_s)|F(0,C_s)|_{\omega_c} \quad (2.10d)$$

and $I(C^f,C_s,h,L)$ is given by (2.6d). Thus (2.10a) reduces to (2.8a) provided that one interchanges the locations of the source and the receiver (2.7) and the solutions derived from the impedance boundary conditions are also consistent with reciprocity. It should be pointed out, however, that using the impedance boundary condition one obtains an extraneous coupling term $D(C^f,C_s)$ [6], which for moderately smooth boundaries is proportional to $Z_s(dh/dx)^2$. The term $D(C^f,C_s)$ has no counterpart in the exact analysis [4] and is therefore neglected in the present derivations.

Using a physical-optics- or Kirchoff-type approximation for the surface wave on the boundary $y = h(x)$, for $x > x_0$

$$H_{zs}(x,y) = H_s^i(x,y)$$
$$= \frac{Ki\omega\varepsilon_0}{n(1 - 1/\varepsilon_r^2)}\exp[-i(\beta_s(x - x_0) + u_{0s}(y + y_0))] \quad (2.11a)$$

and

$$-i\omega\varepsilon\bar{a}_z \cdot (\bar{n} \times \bar{E}) = \frac{\partial H_{zs}(x,y)}{\partial n}$$
$$= -i[\bar{n} \cdot (\beta_s\bar{a}_x + u_{0s}\bar{a}_y)]H_s^i(x,y). \quad (2.11b)$$

Thus on substituting (2.11) into the Helmholtz equation [2] one obtains $H_{zs}^r = 0$ for the physical optics approximation to the scattered radiation (far) field. Thus the physical optics approach fails to determine the scattered radiation fields in the Fraunhofer zone, when the incident field is a surface wave, because the physical optics approximation for the surface wave at the boundary is not appropriate.

III. Full-Wave Solutions for the Scattered Lateral Wave Excited by Line Sources at Large Distances from a Rough Surface and the Reciprocal Problem

In addition to the scattered radiation field and the scattered surface wave (Section II), a plane wave incident upon a rough surface will couple into a lateral wave [4]. Thus the scattered vertically polarized lateral wave at (x,y) due to a magnetic line source of intensity K (volts) located at (x_0,y_0) in medium 0 (Fig. 1) is

$$H_{z0}^l(x,y) = |H_0^i|\exp[-ik_0\rho_0]\frac{1}{2\pi}\frac{(2L/\lambda_c)}{(L_1/\lambda_c)^{3/2}}F(C^\delta,C^i)$$
$$\cdot I(C^\delta,C^i,h,L)\exp[-i(k_1 L_1 + k_0 L_\rho)] \quad (3.1a)$$

where

$$F(C^\delta,C^i) = (nC_1^i C_0^\delta + S_0^i S_0^\delta)/(C_0^i + C_1^i/n)n^{3/2}\varepsilon_r \quad (3.1b)$$

and

$$I(C^\delta,C^i,h,L) = \frac{1}{2L}\int_{-L}^{L}\exp[iu_0^i h + i(\beta^\delta - \beta^i)x]\,dx \quad (3.1c)$$

in which λ_c is the free-space wavelength at the carrier frequency ω_c:

$$\beta^\delta = k_0 S_0^\delta = k_1 S_1^\delta = k_1 = k_0 n$$
$$u_0^\delta = k_0 C_0^\delta = k_0\sqrt{1 - n^2}$$
$$u_1^\delta = k_1 C_1^\delta = 0. \quad (3.2)$$

The parameters for the incident wave are the same as in Section II, (2.1d) and (2.4b). The lateral waves are of practical significance only for low-loss medium 1 where

$$n = n' - in'' = S_0^\delta = \sin\delta = \sin(\delta' - i\delta'')$$
$$\simeq \sin\delta' - i\delta''\cos\delta' \quad (3.3)$$

thus

$$u_0^\delta y + \beta^\delta x = k_0[\cos(\delta)y + \sin(\delta)y\tan(\delta) + \sin(\delta)(x - y\tan\delta)]$$
$$\simeq k_0[y/\cos\delta' + n(x - y\tan\delta')]$$
$$= k_0 L_\delta + k_1 L_1 \quad (3.4a)$$

and the distances L_δ and L_1 are (Fig. 1)

$$L_\delta = y/\cos\delta' \quad \text{and} \quad L_1 = x - y\tan\delta'. \quad (3.4b)$$

Equation (3.1a) is valid for $|k_1|L_1 \gg 1$ in view of the steepest descent method used to derive it. For a plane wave incident at the critical angle $\theta_0^i = \delta'$

$$F(C^\delta, C_0^i = \cos\delta')|_{\omega_c} = \left|\frac{\{[1-(n'/n)^2]^{1/2}\cos\delta + n'\}/n^{3/2}}{n[1-(n')^2]^{1/2} + [1-(n'/n)^2]^{1/2}}\right|_{\omega=\omega_c} \quad (3.5a)$$

$$H_{zl} = H_l^i(x,y) = \frac{-K\omega_c\varepsilon_0\left(\frac{\omega_c}{i\omega}\right)^{1/2}}{(1-n^2)2(2\pi)^2 n^{3/2}} \frac{\exp[-ik_0(y+y_0)/\cos\delta' - ik_1(x - x_0 - (y+y_0)\tan\delta')]}{[\{x - x_0 - (y+y_0)\tan\delta'\}/\lambda_c]^{3/2}} \quad (3.8a)$$

and the function F (3.1b) is normalized such that

$$F_N(C^\delta, C^i) = F(C^\delta, C^i)/|F(C^\delta, C_0^i = \cos\delta')|_{\omega_c}. \quad (3.5b)$$

In (3.1a) the input term $|H_0^i|\exp[-ik_0\rho_0]$ is the incident radiation field and the output term $\exp[-i(k_1L_1 + k_0L_\delta)]$ is the scattered lateral wave (see Fig. 1). As in Section II, the coupling is represented by the factors $F(C^\delta, C^i)$ and $I(C^\delta, C^i, h, L)$.

Similarly, for a backward-traveling lateral wave of complex magnitude H_{l0} at the origin, the scattered radiation field at the observation point (x,y) is

$$H_{zl}^r = -H_{l0}\left(\frac{i\omega}{\omega_c}\right)^{1/2} 2k_{0c}L(1-n^2)n^{3/2} \cdot F(C^f, C^\delta)I(C^f, C^\delta, h, L)\frac{\exp[-ik_0\rho]}{[2\pi k_{0c}\rho]^{1/2}} \quad (3.6a)$$

where

$$H_{l0} = \frac{-K\omega_c\varepsilon_0\left(\frac{\omega_c}{i\omega}\right)^{1/2}\exp\left[-ik_0\left(\frac{y_0}{\cos\delta'}\right) - ik_1(x_0 - y_0\tan\delta')\right]}{(1-n^2)2(2\pi)^2 n^{3/2}[(x_0 - y_0\tan\delta')/\lambda_c]^{3/2}} \quad (3.6b)$$

$$F(C^f, C^\delta) = (nC_1^iC_0^\delta - S_0^fS_0^\delta)/(C_0^i + C_1^i/n)n^{3/2}\varepsilon_r \quad (3.6c)$$

$$I(C^f, C^\delta, h, L) = \frac{1}{2L}\int_{-L}^{L}\exp[iu_0^f h + i(\beta^\delta + \beta^f)x]\,dx \quad (3.6d)$$

and the locations of the source and observation points are interchanged. Thus

$$\rho_0 \to \rho \qquad x \to x_0 \qquad y \to y_0 \qquad \theta_0^i \to -\theta_0^f. \quad (3.7)$$

Hence (3.6) and (3.1) are consistent with the reciprocity relationship. In (3.6), the input term is the incident lateral wave H_{l0} and the output term $\exp[-ik_0\rho]/[2\pi k_{0c}\rho]^{1/2}$ is the scattered radiation field. The expression between these terms $F(C^f, C^\delta)I(C^f, C^\delta, h, L)$ represents the coupling phenomenon.

Using the constant surface impedance concept, the lateral-wave contribution to the total field due to the branch cut Im $(u_1) = 0$ vanishes. Thus if the lateral wave constitutes a significant part of the total field the surface impedance concept cannot be used [3].

Furthermore, a physical-optics- or Kirchoff-type approximation for the lateral wave on the boundary $y = h(x)$ for $|k_1|(x - x_0 - (y + y_0)\tan\delta') \gg 1$, is

and

$$-i\omega\varepsilon\bar{a}_z \cdot (\bar{n} \times \bar{E}) = \frac{\partial H_{zl}}{\partial n} = -i[\bar{n} \cdot (\beta^\delta\bar{a}_x + u_0^\delta\bar{a}_y)]H_l^i(x,y). \quad (3.8b)$$

On substituting (3.8) into the Helmholtz equation [2], $H_{z1}^r = 0$ for the physical optics approximation to the scattered radiation field. Thus the physical optics approximation for the incident lateral wave at the boundary cannot be used to determine the scattered radiation fields in the Fraunhofer zone.

IV. Coupling Between the Lateral Waves and the Surface Waves Over a Rough Surface—Full-Wave Solutions

In addition to coupling between the radiation fields and the surface and lateral waves considered earlier, the excitation of a scattered surface wave due to an incident lateral wave over a rough surface and the reciprocal problem (Fig. 2) is considered here in detail.

The expression for the incident lateral wave near the boundary for

$$|k_1|(x - x_0 - y_0\tan\delta') \gg 1,$$
$$x_0 < -L, \quad \text{and} \quad |n| < 1 \text{ is [3]}$$

$$H_l(x,y) = \frac{-Ki\omega\varepsilon_0\exp[-iu_0^\delta y_0 - i\beta^\delta(x - x_0)]\exp(-iu_0h)\psi_1(u,y)}{(1-n^2)2(2\pi)^{1/2}[i\beta^\delta(x - x_0 - y_0\tan\delta')]^{3/2}\psi_1(u,h)} \equiv a_1^i(x,u^\delta)\psi_1(u^\delta,y) \quad (4.1)$$

in which $\psi_1(u,y)$ is the basis function associated with the contribution from the branch cut Im $(u_1) = 0$ [3]. Thus on applying the orthogonality relationships between the basis functions, the lateral-wave transform $H_1(x,u)$ is

$$H_1(x,u) = a_1^i(x,u^\delta)\delta(u - u^\delta)\delta_{p,1}, \qquad p = 0, 1, \text{ or } S \quad (4.2)$$

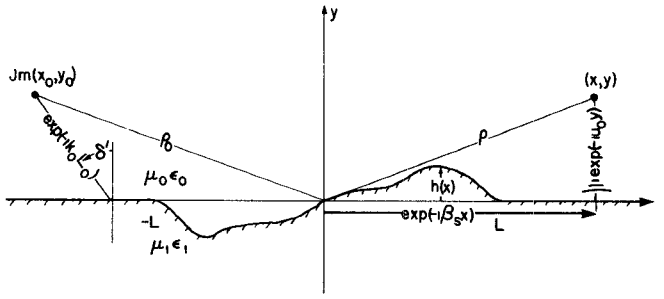

Fig. 2. The scattered surface wave due to incident lateral waves.

where $a_1(x,u)$ is defined by (4.1) and $\delta(u-u^\delta)$ and $\delta_{p,1}$ are the Dirac and Kronecker delta functions, respectively. The differential equation for the forward-scattered surface-wave amplitude $a_s(x,u_s)$ due to an incident lateral wave (4.2) is [4].

$$-\frac{d}{dx}a_s(x,u_s) - i\beta_s a_s(x,u_s) \simeq S_{s1}^{BA}(u_s,u^\delta)a_1(x,u^\delta) \quad (4.3a)$$

in which the transmission scattering coefficient S_{s1}^{BA} is

$$S_{s1}^{BA}(u_s,u^\delta) = \frac{\psi_1(u^\delta,h)\Psi_s(u_s,h)h'}{2\omega\varepsilon_0(\beta^\delta-\beta_s)} \cdot [\beta^\delta\beta_s + u_0^\delta u_{1s}]\left[1-\frac{1}{\varepsilon_r}\right] \quad (4.3b)$$

and $\Psi_s(u_s,h)$ is the basis function for the surface waves [3]. Thus

$$a_s(x,u_s) = -\exp(-i\beta_s x)\int_{-L}^{L} S_{s1}^{BA}(u_s,u^\delta) \cdot a_1^i(x',u^\delta)\exp(i\beta_s x')\,dx' \quad (4.4a)$$

and the scattered surface wave for $x > L$ and $y > h$ is

$$H_l^s(x,y) = a_s(x,u_s)\Psi_s(u_s,h)\exp(-iu_{0s}y). \quad (4.4b)$$

Hence,

$$H_l^s(x,y) = K\exp(-i\beta_s x - iu_{0s}y)\exp[-iu_0^\delta y_0 + i\beta^\delta x_0] \cdot (\beta^\delta\beta_s + u_0^\delta u_{1s})\left(1-\frac{1}{\varepsilon_r}\right)[\Psi_s(u_s,h)]^2 \cdot \frac{i}{(1-n^2)4(2\pi)^{1/2}(\beta^\delta-\beta_s)} \cdot \int_{-L}^{L}\frac{h'\exp[-iu_0^\delta h - i(\beta^\delta-\beta_s)x']\,dx'}{[i\beta^\delta(x'-x_0-y_0\tan\delta')]^{3/2}} \quad (4.5)$$

and on integrating by parts and neglecting edge effects

$$H_l^s(x,y) = \frac{Ki\omega\varepsilon 2\pi}{(-2\pi ik_1x_0)^{3/2}}\exp[-i(u_0^\delta y_0 - \beta^\delta x_0)] \cdot ik_0 LF(u_s,u^\delta)I(u_s,u^\delta,h,L)\exp[-i(u_{0s}y+\beta_{0s}x)] \quad (4.6a)$$

where

$$I(u_s,u^\delta,h,L) = \frac{1}{2L}\int_{-L}^{L}\frac{\exp[-iu_0^\delta h - i(\beta^\delta-\beta_s)x']}{[1+(y_0\tan\delta'-x')/x_0]^{3/2}} \cdot \left[1+\frac{3}{2i(\beta^\delta-\beta_s)(x'-x_0-y_0\tan\delta')}\right]dx' \quad (4.6b)$$

and

$$F(u_s,u^\delta) = [C_0^\delta+1][\varepsilon_r/(1-\varepsilon_r^2)]^{3/2}. \quad (4.6c)$$

Thus, in (4.6b), the input term is the incident lateral wave and the output term is the scattered surface wave with the coupling represented by $F(u_s,u^\delta)I(u_s,u^\delta,h,L)$ (see Fig. 2).

For the reciprocal case, the scattered lateral wave due to a backward-traveling surface wave of complex magnitude H_{s0} at the origin, (2.6b), is obtained by interchanging the locations of the source and the receiver. Thus for $x < -L$, $y > h$, and $|k_1(x+y\tan\delta'-L)| \gg 1$,

$$H_s^l(x,y) = Ki\omega\varepsilon 2\pi\exp[-i(u_{0s}y_0+\beta_s x_0)] \cdot ik_0LF(u^\delta,u_s)I(u^\delta,u_s,h,L) \cdot \frac{\exp[-i(u_0^\delta y-\beta^\delta x)]}{(2\pi ik_1x)^{3/2}} \quad (4.7a)$$

where

$$I(u^\delta,u_s,h,L) = \frac{1}{2L}\int_{-L}^{L}\frac{\exp[-iu_0^\delta h - i(\beta^\delta-\beta_s)x']}{[1+(y\tan\delta'-x')/x]^{3/2}} \cdot \left[1+\frac{3}{2i(\beta^\delta-\beta_s)(x'-x-y\tan\delta')}\right] \quad (4.7b)$$

and

$$F(u^\delta,u_s) = F(u_s,u^\delta). \quad (4.7c)$$

Hence (4.6) converts to (4.7) on interchanging x_0,y_0 with x,y and the solutions are consistent with the reciprocity relationship. In (4.7) the input term is the incident surface wave and the output term is the scattered lateral wave and $F(u^\delta,u^s)I(u^\delta,u^s,h,L)$ represents the coupling.

The analysis presented in this section is relevant to problems of propagation near the rough surface of the sea, the ionosphere, and in dielectric waveguides.

When the source and the observation point are near the air–ground interface and

$$\left|\frac{x_0}{L}\right| \gg 1 \quad \text{and} \quad \left|\frac{x}{L}\right| \gg 1$$

$$I(u_s,u^\delta,h,L) \simeq \frac{1}{2L}\int_{-L}^{L}\exp[-iu_0^\delta h - i(\beta^\delta-\beta_s)x']\,dx' \quad (4.8a)$$

and

$$I(u^\delta,u_s,h,L) = I(u_s,u^\delta,h,L). \quad (4.8b)$$

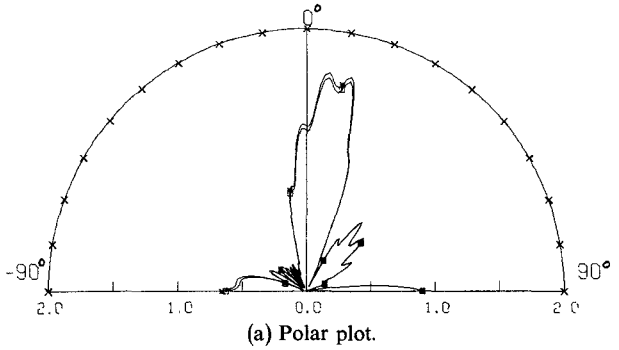

(a) Polar plot.

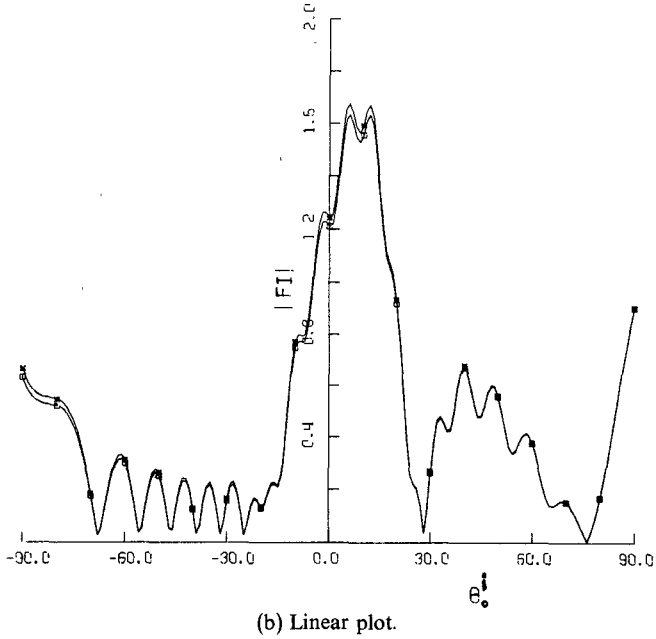

(b) Linear plot.

Fig. 3. $|F_N I|$ function of θ_0^i for $k_0 h_{max} = 20$, $L = 10\lambda_0$, and $\varepsilon_r = 10 - i10$. Solution I: □. Solution II: *. Plane-wave–surface-wave coupling.

Thus the coupling between the lateral wave and the surface wave is large when over a significant portion of the rough surface

$$u_0^\delta \, dh/dx + \beta^\delta - \beta_s \simeq 0. \tag{4.9a}$$

Using (2.4a) and (3.2), (4.9a) reduces to

$$\frac{dh}{dx} = \left(\sqrt{\frac{\varepsilon_r}{1+\varepsilon_r}} - \sqrt{\varepsilon_r}\right) \Big/ \sqrt{1-\varepsilon_r}$$
$$= \left(\frac{\varepsilon_r}{1-\varepsilon_r^2}\right)^{1/2} - \left(\frac{\varepsilon_r}{1-\varepsilon_r}\right)^{1/2}. \tag{4.9b}$$

V. Illustrative Examples

In this section some numerical results are presented for the scattered surface waves and lateral waves due to plane waves incident at angles θ_0^i over rough surfaces. In view of the reciprocity relationships these results also give the scattered radiation patterns as functions of θ_0^f due to incident surface waves and incident lateral waves. In addition $F_N(C_s,C^i)$, $F_N(C^\delta,C^i)$ are plotted as functions of θ_0^i for various values of ε_r. For the case of the scattered radiation field due to incident surface waves (and the reciprocal case)

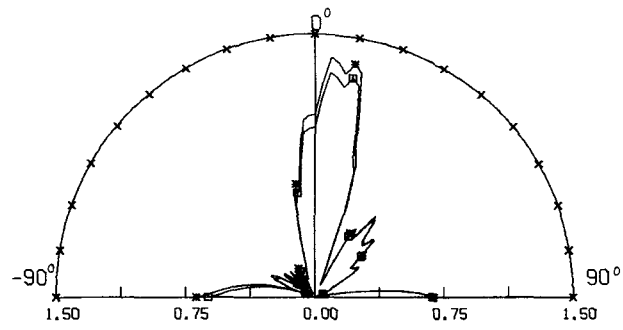

Fig. 4. $|F_N I|$ function of θ_0^i for $k_0 h_{max} = 20$, $L = 10\lambda_0$, and $\varepsilon_r = 10 - i$. Solution I: □. Solution II: *. Plane-wave–surface-wave coupling.

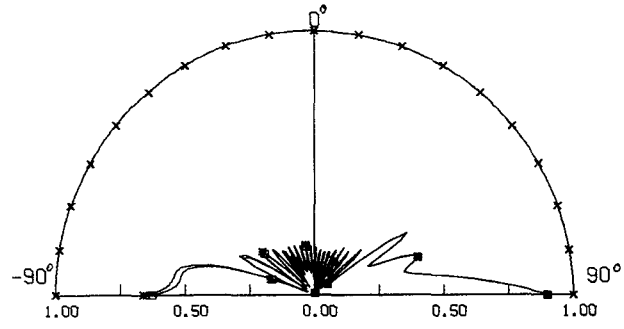

Fig. 5. $|F_N I|$ function of θ_0^i for $k_0 h_{max} = 2$, $L = 10\lambda_0$, and $\varepsilon_r = 10 - i10$. Solution I: □. Solution II: *. Plane-wave–surface-wave coupling.

both solution I (2.5b) and solution II (2.8b) are used for $F_N(C_s,C^i)$, thus the surface impedance approximation to the problem is also examined.

The interface between the two media is assumed to be

$$h(x) = h_{max}[1 + \cos(\pi x/L)]/2, \qquad -L \le x \le L \tag{5.1}$$

with $2L = 10\lambda_c$ and ω is set equal to ω_c.

In Figs. 3 and 4 $|F_N(C_s,C^i)I(C_s,C^i,h,L)|$, the magnitude of the scattered surface waves, is plotted as a function of $-\pi/2 \le \theta_0^i \le \pi/2$ for $k_0 h_{max} = 20$, with $\varepsilon_r = (10 - i10)$ and $\varepsilon_r = (10 - i)$, respectively, and in Fig. 5 for $k_0 h_{max} = 2$ and $\varepsilon_r = (10 - i10)$. Both a polar and a linear plot are given for the scattered surface waves in Fig. 3. In all subsequent examples only the polar plots of the scattered surface waves are given. When the relative permittivity is large, $|\varepsilon_r| \gg 1$, the surface impedance approximation is in very good agreement with the two-media rigorous analysis (Fig. 3). The discrepancy between the solutions based on the impedance approximation (2.8b) and the two-media analysis (2.5b) increases as θ_0^f decreases from $\pi/2$ to $-\pi/2$ (Fig. 4). This discrepancy also increases as $|\varepsilon_r|$ decreases. For small values of $k_0 h$ the scattered surface wave is largest for grazing incidence, $\theta_0 \to \pi/2$ ($k_0 h = 2$, Fig. 5). For large values of $k_0 h_{max}$ ($k_0 h_{max} = 20$), coupling into the surface wave is largest for near normal incidence, $\theta_0^i \simeq 0$ (Figs. 3 and 4). Thus on considering the reciprocal problem, the scattered radiation field is largest when $\theta_0^f \to \pi/2$ for $k_0 h_{max} = 2$. However, for $k_0 h_{max} = 20$ the scattered radiation fields are largest in the direction $\theta_0^f \simeq 0$. Thus these results can be used to determine optimum coupling into and out of surface-wave structures (dielectric waveguides).

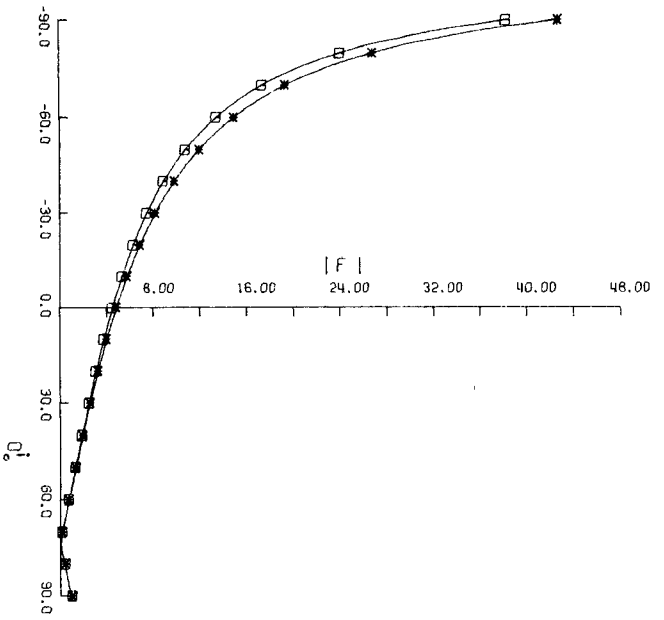

Fig. 6. $|F_N|$ function of θ_0^i for $\varepsilon_r = 10 - i$. Solution I: □. Solution II: *. Plane-wave–surface-wave coupling.

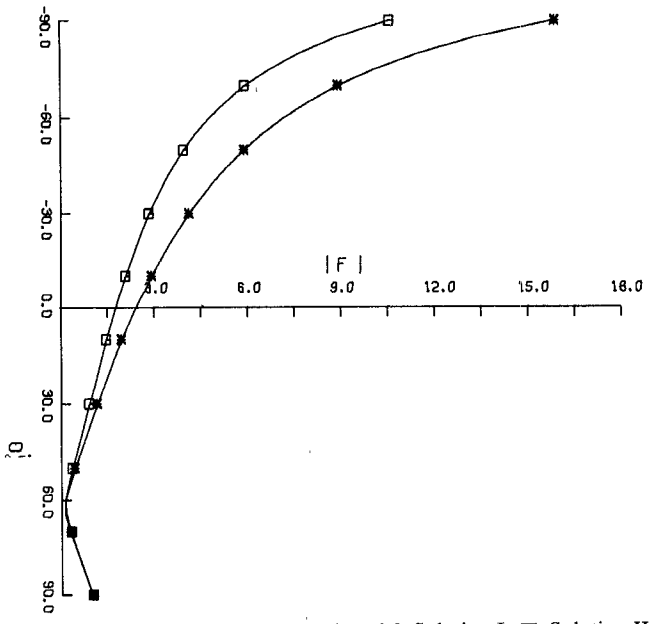

Fig. 7. $|F_N|$ function of θ_0^i for $\varepsilon_r = 3 - i0.9$. Solution I: □. Solution II: *. Plane-wave–surface-wave coupling.

In Figs. 6 and 7 the normalized functions $F_N(C_s, C^i)$, (2.5b) and (2.8b), are plotted for $\varepsilon_r = 10 - i$ and $\varepsilon_r = 3 - i0.9$, respectively. Thus for $|\varepsilon_r| > 10$, the surface impedance approximation is in good agreement with the rigorous two-media analysis, except for $\theta_0^i \to -\pi/2$. This agreement deteriorates as $|\varepsilon_r|$ decreases. The minima of the function $F(C_s, C^i)$, (2.1b), occurs when

$$S_0^i = C_1^i. \tag{5.2}$$

Equation (5.2) is satisfied when $\tan \theta_0^i = n' \equiv \tan \theta_0^B$, where θ_0^B is the Brewster angle. Thus dielectric waveguides cannot be excited efficiently at the Brewster angle.

In Figs. 8 and 9 the magnitude of the scattered lateral waves $|F_N(C^\delta, C^i)I(C^\delta, C^i, h, L)|$, (3.1), is plotted as a function of the angle of incidence $(-\pi/2 \le \theta_0^i \le \pi/2)$ of the plane waves for $k_0 h_{\max} = 20$ and $\varepsilon_r = 1 - X/(1 - iZ)$ with $X = 0.5$, $Z = 0$ and $X = 0.5$, $Z = 0.1$, respectively. In Fig. 10, $k_0 h_{\max} = 2$ and $\varepsilon = 1 - X = 0.5$. Thus for small values of $k_0 h$ (Fig. 10), the scattered lateral wave is largest when the incident plane wave is at the critical angle for total internal reflection $\theta_0^i = \delta' = 45°$ (3.3). For large values of $k_0 h$ (Figs. 8 and 9) strong coupling into the lateral waves occurs for several directions between 45 and 75°. Thus for the reciprocal case the scattered radiation pattern due to an incident lateral wave has only one major lobe in the direction of the critical angle $\theta_0^f = \delta' = 45°$, for $k_0 h_{\max} = 2$. For $k_0 h_{\max} = 20$ the radiation pattern has several major lobes between $\theta_0^f = \delta'$ and 75°. When dissipation is accounted for in medium 2 ($Z = 0.1$, Fig. 9), the lobe structure of the scattered lateral wave (or the reciprocal scattered radiation pattern) becomes more diffuse and coupling between the lateral waves and plane waves of grazing incidence increases.

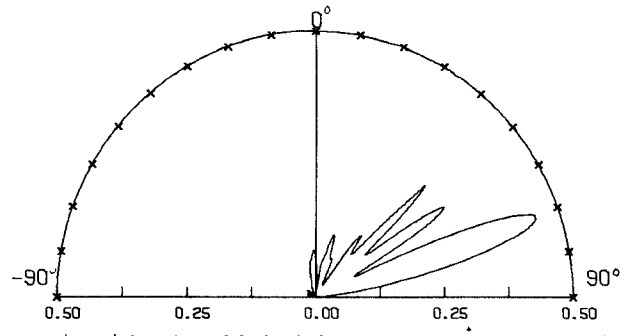

Fig. 8. $|F_N I|$ function of θ_0^i for $k_0 h_{\max} = 20$, $L = 10\lambda_0$, $\varepsilon_r = 0.5$. Plane-wave–lateral-wave coupling.

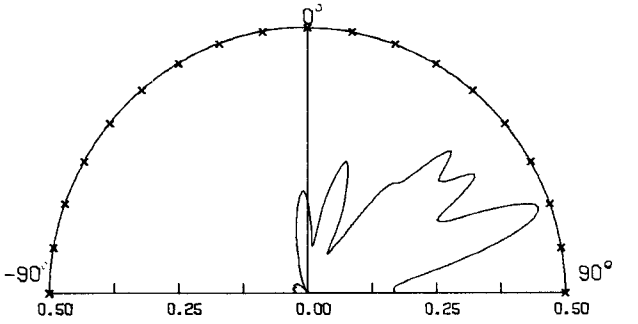

Fig. 9. $|F_N I|$ function of θ_0^i for $k_0 h_{\max} = 20$, $L = 10\lambda_0$, $\varepsilon_r = 1 - 0.5/(1 - 0.1i)$. Plane-wave–lateral-wave coupling.

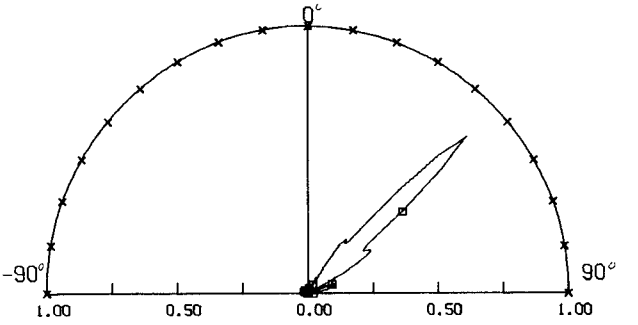

Fig. 10 $|F_N I|$ function of θ_0^i for $k_0 h_{\max} = 2$, $L = 10\lambda_0$, $\varepsilon_r = 0.5$. Plane-wave–lateral-wave coupling.

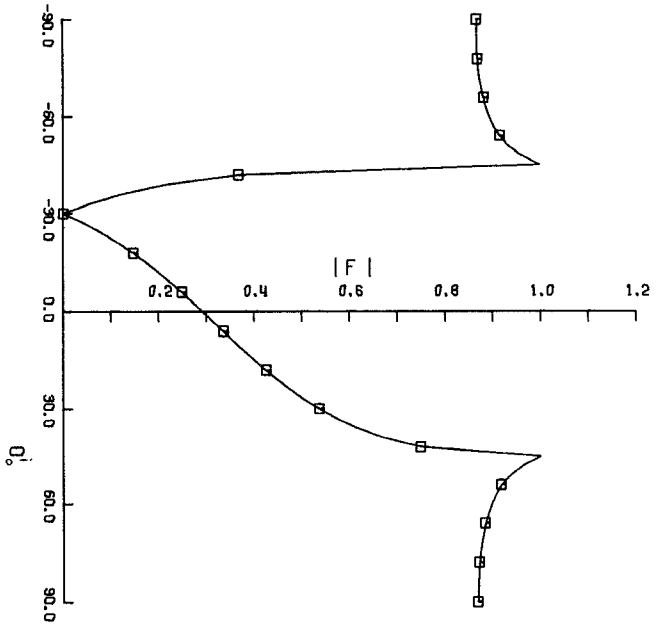

Fig. 11. $|F_N|$ function of θ_0^i for $\varepsilon_r = 0.5$. Plane-wave–lateral-wave coupling.

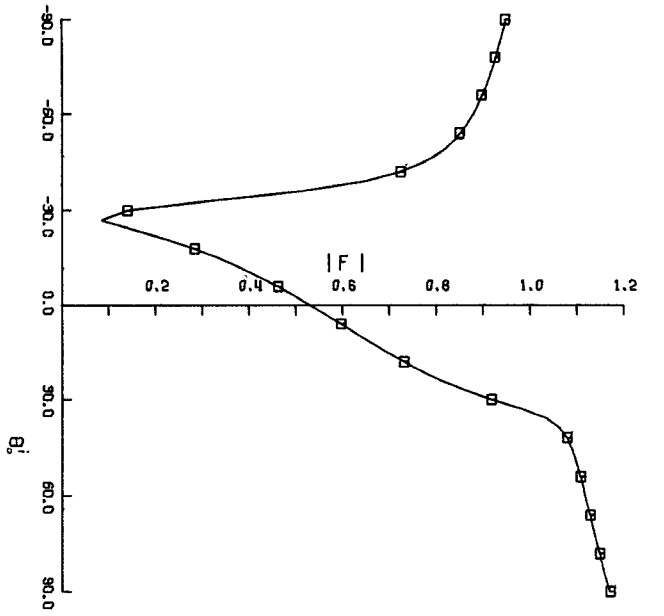

Fig. 12. $|F_N|$ function of θ_0^i for $\varepsilon_r = 1 - 0.7/(1 - 0.1i)$. Plane-wave–lateral-wave coupling.

In Figs. 11 and 12, $|F_N(C^\delta, C^i)|$, (3.5b), is plotted for $\varepsilon_r = 0.5$ and $\varepsilon_r = 1 - X/(1 - iZ)$ with $X = 0.7$, $Z = 0.1$, respectively. For nondissipative media $F(C^\delta, C^i)$, (3.1b), vanishes for

$$C_1^i C_0^\delta + S_0^i = 0. \tag{5.3a}$$

This accounts for the sharp null in Fig. 11 at

$$\sin \theta_0^i = -\sin \delta \cos \delta = -n(1 - n^2)^{1/2}, \qquad \theta_0^i = -30°. \tag{5.3b}$$

For dissipative media (Fig. 12) the minima occurs at

$$\sin \theta_0^i = -\sin \delta' \cos \delta', \qquad \theta_0^i \simeq -27°. \tag{5.3c}$$

This is the principal reason why the forward-scattered lateral waves are very small for $\theta_0^i < 0$ even for large values of $k_0 h$.

VI. Concluding Remarks

In this paper full-wave solutions are presented for the guided surface waves and lateral waves excited at the irregular boundary between two semi-infinite media. The explicit solutions are presented in a form that can be readily used. Thus the incident wave, which could be the radiation field, the surface wave, or the lateral wave is related to the scattered (output) field through the factors F and I, which depend on the electrical and the geometrical parameters of the irregular boundary.

The validity of the surface impedance approximation is examined for the case of coupling between the radiation fields and the surface waves. It is shown that the impedance boundary condition yields results that are in good agreement with the rigorous two-media analysis provided that $|\varepsilon_r| \gg 1$. The discrepancies between the two results increases as $|\varepsilon_r|$ decreases and as $\theta_0^i \to \pi/2$. There is a sharp minima in the function $F(C_s, C^i)$ when $\theta_0^i = \theta_0^B$ (the Brewster angle). Thus coupling between surface waves and plane waves incident at the Brewster angle $\theta_0^i = \theta_0^B$ is negligible. It is interesting to note that at the Brewster angle $R_0(u^i) = 0$ and that $I/R_0(u_s) = 0$ for the surface waves. However, both the plane waves at the Brewster angle and the surface waves are characterized by the same wave parameter β.

For the examples considered in Section V coupling between the incident plane waves and surface waves is maximum for $\theta_0^i = \pi/2$ when $k_0 h_{\max} = 2$. However, for $k_0 h_{\max} = 20$, the coupling is maximum for $\theta_0^i \simeq 0$.

Similarly, it is shown that for $k_0 h_{\max} = 2$ coupling between the incident plane waves and the lateral wave is maximum for a plane wave incident at the critical angle for total internal reflection $\theta_0^i = \delta'$. For $k_0 h_{\max} = 20$, however, there are several directions between $\theta_0^i = \delta'$ and $\theta_0^i \to \pi/2$ for which the coupling is strong. Thus for the reciprocal problem, the scattered radiation pattern has several large lobes for $k_0 h_{\max} = 20$ and only one in the direction of the critical angle $\theta_0^f = \delta'$ when $k_0 h_{\max} = 2$. The surface impedance approximation cannot be used to determine the coupling between the plane waves and the lateral waves.

Coupling between the lateral waves and the surface waves are also considered in detail and the results are shown to be consistent with reciprocity. The region of the rough surface where most of the contribution to coupling occurs is also specified (4.9b). In this case too, the impedance boundary condition cannot be used.

For all the cases considered in this paper the physical-optics- or Kirchoff-type approximation for the boundary conditions cannot be used to obtain the scattered surface

waves, the lateral waves, or even the scattered radiation (far) fields due to incident surface or lateral waves.

This work is of particular interest in propagation problems when either the transmitter or receiver are near the irregular boundary. It is applicable to problems of coupling into and out of surface-wave structures. The electromagnetic problems considered here and the dual problems in acoustics are relevant to geophysical prospecting and active remote sensing.

Acknowledgment

The computations were performed by B. S. Agrawal and the manuscript was prepared by Mrs. E. Everett.

References

[1] S. O. Rice, "Reflection of electromagnetic waves from slightly rough surfaces," *Communication on Pure and Applied Mathematics*, vol. IV, no. 3, pp. 351–378, 1951.
[2] P. Beckmann and A. Spizzichino, *The Scattering of Electromagnetic Waves from Rough Surfaces*. New York: Macmillan Co., 1963.
[3] E. Bahar, "Generalized Fourier transforms for stratified media," *Canadian J. Physics*, vol. 50, no. 24, pp. 3123–3131, 1972.
[4] ——, "Radio wave propagation in stratified media with nonuniform boundaries and varying electromagnetic parameters, full wave analysis," *Canadian J. Physics*, vol. 50, no. 24, pp. 3132–3142, 1972.
[5] ——, "Radio wave propagation over a rough variable impedance boundary: Part I—Full wave analysis," *IEEE Trans Antennas Propagat.*, vol. AP-20, pp. 354–362, 1972.
[6] ——, "Radio wave propagation over a rough variable impedance boundary: Part II—Application of full wave analysis," *IEEE Trans. Antennas Propagat.*, vol. AP-20, pp. 362–368, 1972.

Traveling Waves in Coupled Yagi Structures

CHUN C. LEE AND LIANG C. SHEN, SENIOR MEMBER, IEEE

Abstract—**The propagating mode in a coupled Yagi-Uda array of cylindrical wires is studied. The current distribution in each element, the phase velocity; and the cutoff frequency of the propagating mode are found, firstly by a numerical method and secondly by a method based on an assumed current distribution. These two methods yield essentially the same results. Mutual coupling between the arrays is studied. The characteristics of the propagating waves in the coupled Yagi-Uda structure have been measured. The experimental K-β diagram of the waves is obtained and is found to be in good agreement with the theory.**

I. Introduction

A TRAVELING WAVE can be supported on a periodic array of identical wires or strips that are equally spaced and perpendicular to the direction of the array. The existence of the traveling wave in such a structure, known as an infinitely long Yagi–Uda array, has been confirmed by theory and by experiments [1]–[5]. The traveling wave is a slow wave, that is, the phase velocity is smaller than the velocity of a uniform plane wave in the same medium in the absence of the structure. When one of the elements of the array is excited, currents on the parasitic elements are induced by a mutual coupling effect, resulting in a traveling wave. These currents have progressive phase shifts. The amount of phase shift and the distribution of the current in each element are determined by the array geometry. This information is useful when the structure is employed for uses such as millimeter waveguides or antennas [6].

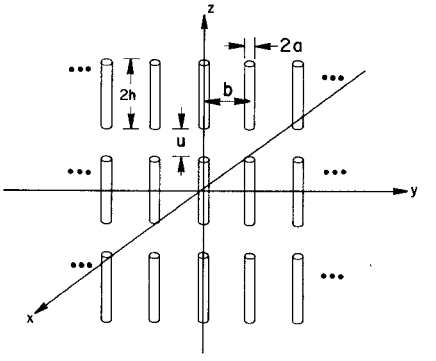

Fig. 1. Coupled three-row Yagi–Uda structure.

In order to carry more power or to divide it equally among several branches when the structure is used to transmit millimeter waves, several similar ones may be arranged in parallel in the same plane, as shown in Fig. 1. When used as an antenna, this arrangement could produce an elevation beamwidth that is narrower than that of a single Yagi array.

The present study also indicates the level of mutual coupling between two closely spaced Yagi structures when they are used separately for millimeter-wave transmission.

Little work has been done on the subject of coupled Yagi arrays. A study was made not long ago to obtain the phase velocity of a traveling wave on two Yagi arrays arranged in

Manuscript received January 13, 1977; revised April 8, 1977. This work was supported by the National Science Foundation under Grants ENG 74-13705 and ENG 76-17596.

C. C. Lee was with the Department of Electrical Engineering, University of Houston, Houston, TX. He is now with the Airtron Division, Litton System, Inc., Morris Plains, NJ 07950.

L. C. Shen is with the Department of Electrical Engineering, University of Houston, Houston, TX 77004.